Secondary Ion Mass Spectra of Apatites*

A. Lodding, S. J. Larsson, and H. Odelius

Materials Science Centre, Chalmers University of Technology, 402 20 Gothenburg, Sweden

Z. Naturforsch. **33 a**, 697–708 (1978); received April 7, 1978

The detection sensitivities and the possibilities of quantification in the ion probe analysis of microelements in tooth and bone mineralized tissue are limited partly by selective ionization yields, partly by the complicated intrinsic mass spectra of the apatite matrix. Such intrinsic spectra have been recorded for hydroxy-, fluor- and chlorapatite. The limits of analysis have been examined for most of the elements in the periodic table. With a routine SIMS technique developed for the study of mineralized tissues, the lowest concentrations for semi-quantitative measurement have been assessed to lie below 10 wt ppm for at least 20 elements and below 100 wt ppm for another 25 to 30 trace elements in apatites.

Introduction

The success of recent applications of the ion probe technique in the investigation of microelement distributions in biological mineralized tissue [1] – [6] motivates a detailed examination of the SIMS detection limits for various impurities in apatite matrices. In practice, detection sensitivity is given not only by the formation probability of each ionic species, but more importantly by the spectral background at the relevant mass numbers. One therefore wishes to perform as quantitative a study as possible of the intrinsic spectra of the pure matrix. Such a study not only facilitates the assessment of practical detection limits, but may also contribute to the understanding of the mechanisms of ionization and clustering in SIMS [7].

In the present work, detailed intrinsic positive and negative mass spectra are presented as measured for pure specimens of hydroxyapatite (HAP), fluorapatite (FAP) and chlorapatite (ClAP). The different ionic species corresponding to the spectral peaks are identified. Mass numbers of low intrinsic spectral background are selected as suitable for the detection of impurities. A simplified model of the mechanism of selective ionization is then employed to assess semi-quantitatively the lowest concentrations for the routine analysis of different trace elements in apatite matrices.

Experimental

The ion probe employed in this study was a commercial Cameca IMS 300 analyzer, equipped with an extra electrostatic deflection sector and with an on-line computer for quantitative work. The extra sector makes the instrument double focusing, considerably increasing the available mass resolution as well as the energy window of the secondary ions. The present measuring technique was intended to resemble as closely as possible the standard procedure empirically found [4, 5] to be optimal for the study of biological hard tissue. The utilized mass resolution was of the order of $\Delta m/m \approx 500$. The secondary ions were collected within the energy range 0 – 90 eV. This means that practically all ions were accounted for (as shown in parallel studies of the energy distributions of the principal ion species, to be reported in a forthcoming paper [8]).

The primary ions employed were O^-, for empirical reasons: with negative beams most of the inconveniences of surface charging on non-conductive samples could be minimized. Coating the sample with a metal layer (Au and In) was nevertheless necessary. As another precaution against excessive charging, and also in order to preserve the conditions of point-analysis, a relatively small primary beam, ca 60 μm diam., was used. The primary ion current was of the order of 0.5 μA. The accelerating voltage was 14.5 kV when positive ions were sampled, 5.5 kV for negative spectra. The primary ion incidence was at approx 45°, extraction of secondary ions at right angles to sample surface.

The vacuum in the sample chamber during operation could be assessed to be of the order of 10^{-7} torr, to which contributed the presence of a "cold finger" next to the sample holder. The cold trap action was of particular importance in suppressing spectral contaminations due to hydride, hydroxide and hydrocarbon ions (often a reduction by some 2 orders of magnitude).

* In part presented at the International SIMS Conference, Münster 1977.

The apatite samples employed were the following: a) polycrystalline ($\approx 1\ \mu$m grain size) synthetic HAP [9] of very high purity except 0 – 100 ppm traces of alkali metals, Mg, Sr, Si, F and Cl, which could be determined by macroscopic analysis or by comparative SIMS-analysis; b) crystal of synthetic FAP (Westinghouse), containing less than 10 ppm Na, K, Mg and Cl; and c) crystal of synthetic ClAP (RCA) with less than 10 ppm Na, K, Mg and F, doped with 0.05 wt.% La.

The secondary ion currents of the most intense peaks recorded (^{56}CaO in the positive, $^{63}PO_2$ in the negative spectrum) were of the order of 10^{-12} A, corresponding to a pulse counting rate of $\approx 10^7$ sec^{-1}. The electronic noise level was ≈ 1 sec^{-1}. At each mass number between 1 and 240 (positive spectrum) and between 1 and 130 (neg. sp.) at least 10 pulses were counted. To minimize surface effects, ion currents were first recorded after at least 10 minutes of sputtering in each sample. Currents from these or greater crater depths were found to vary only slowly with time ($\lesssim 20\%$ per hour). The reproducibility of the measured relative currents (normalized to ^{44}Ca in the positive, to ^{31}P in the negative spectrum) was checked repeatedly for several representative peaks, and generally found to lie close to the statistical value.

Results

The mass spectra are shown graphically in Figures 1 – 2. The positive peaks are normalized to the total Ca^+ ion current, negative peaks to P^-. It should be pointed out that when recording negative spectra the bombarding conditions are not the same as when looking at positive ion currents. Nevertheless the primary beam intensity and the sputtering rates are of the same order of magnitude, and the comparison of absolute count rates has yielded the ratio P^-/Ca^+ of ion currents to be approximately 5×10^{-3}.

In Figs. 1 – 2 the actually observed and identifiable contributions of contaminants (such as Na^+, K^+, Mg^+, Sr^+, La^+, C^+, CaC^+, C^-, C_2^-, CN^-) are neglected. The spectra therefore correspond only to intrinsic peaks (except possibly for ^{1}H, where one may not safely exclude a sizable contribution from water present in the primary beam and in residual atmosphere).

Where, in Figs. 1 – 2, certain peaks differ from one type of apatite to the others, this is shown by shaded portions above the open staples (i. e. above the peak level common to all three materials).

For clarity, Figs. 1 – 2 show intrinsic peaks only above a certain height, $M^{\pm}/Ca^+ \gtrsim 10^{-6}$. Smaller peaks, in as far as they are identifiable as intrinsic,

Table 1. Main peaks of intrinsic positive spectra, common to hydroxy-, fluor-, and chlorapatite. Peak heights related to total Ca^+-yield. For HAP, peak heights for oxygen containing ions are higher than the quoted values (add about 8% for each O atom). For minor (isotope) peaks, see Table 5.

Ion species M	Main peak mass nr N	Relative yield M^+/Ca^+ ($\times 10^6$)	Ion species M	Main peak mass nr N	Relative yield M^+/Ca^+ ($\times 10^6$)
O^+	16	800	$Ca_2O_4^+$	144	$\leqq 1.5$
O_2^+	32	25	Ca_3O^+	136	3
P^{+++}	10.33	0.5	Ca_3O_2	152	120
P^{++}	15.5	5.2	$Ca_3O_3^+$	168	32
P^+	31	2400	$Ca_4O_3^+$	208	7.0
P_2^+	62	$\leqq 0.15$	CaP^+	71	310
PO^+	47	2800	$CaPO^+$	87	430
PO_2^+	63	$\leqq 2.0$	$CaPO_2^+$	103	3000
PO_3^+	79	$\leqq 2.5$	$CaPO_3^+$	119	580
P_2O^+	78	$\leqq 1.5$	$CaPO_4^+$	135	$\leqq 0.8$
$P_2O_2^+$	94	$\leqq 0.55$	Ca_2P^+	111	$\leqq 5$
Ca^{++}	20	4600	Ca_2PO^+	127	$\leqq 3$
Ca^+	40	970000	$Ca_2PO_2^+$	143	$\leqq 1$
Ca_2^+	80	1300	$Ca_2PO_3^+$	159	400
Ca_3^+	120	$\leqq 5$	$Ca_2PO_4^+$	175	300
CaO^{++}	28	$\leqq 8$	Ca_3P^+	151	$\leqq 1$
CaO^+	56	75000	Ca_3PO^+	167	$\leqq 3$
CaO_2^+	72	320	$Ca_3PO_2^+$	183	$\leqq 2$
CaO_3^+	88	$\leqq 29$	$Ca_3PO_3^+$	199	$\leqq 0.1$
CaO_4^+	104	$\leqq 15$	$Ca_3PO_4^+$	215	3.5
Ca_2O^+	96	8600	$Ca_3PO_5^+$	231	27
$Ca_2O_2^+$	112	2000	CaP_2^+	102	$\leqq 4$
$Ca_2O_3^+$	128	8	CaP_2O^+	118	$\leqq 5.5$

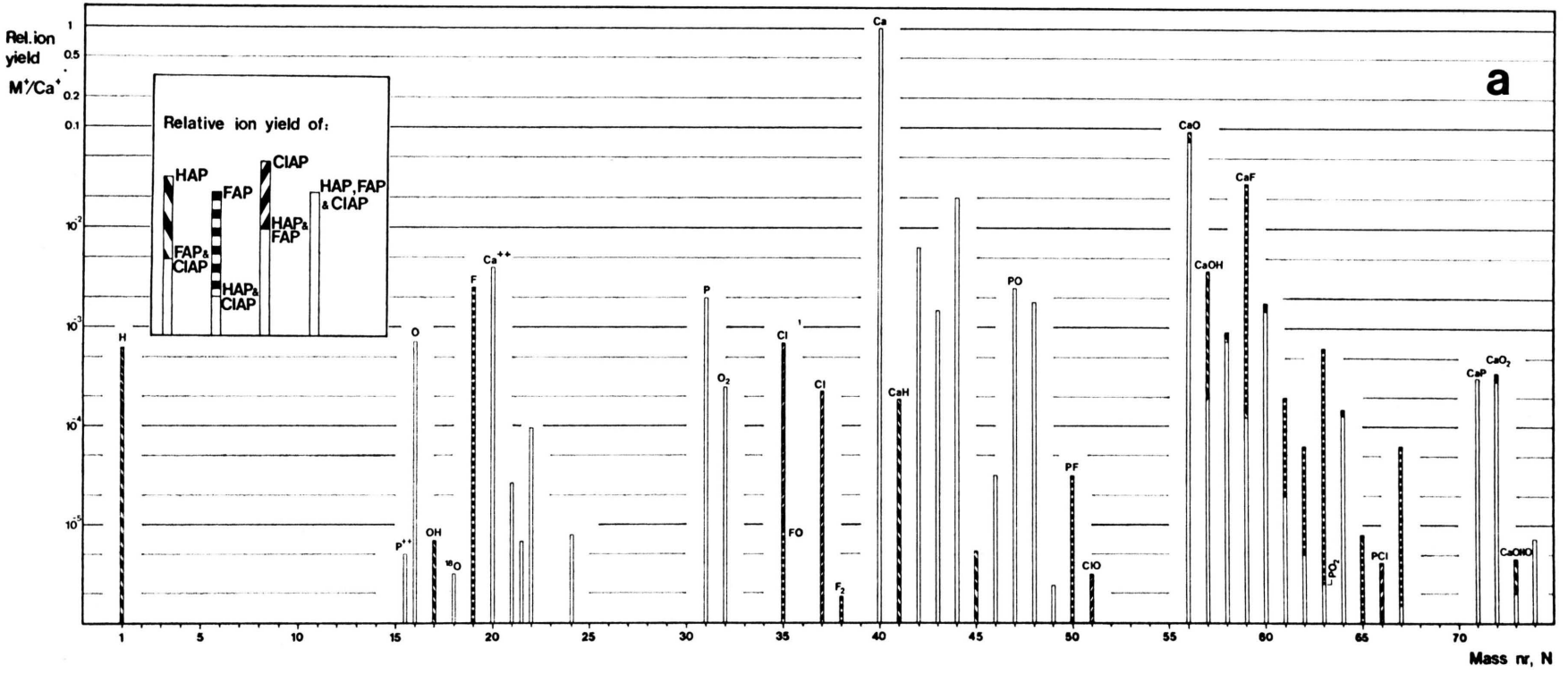
Rel. ion yield M+/Ca++
1
0.5
0.2
0.1
10-2
10-3
10-4
10-5
Relative ion yield of:
HAP
FAP
ClAP
FAP & ClAP
HAP & ClAP
HAP & FAP
HAP, FAP & ClAP
a
H
O
OH
18O
P++
F
Ca++
P
O2
Cl
FO
Cl
F2
Ca
CaH
PO
PF
ClO
CaO
CaOH
CaF
PO2
PCl
CaP
CaO2
CaOHO
1
5
10
15
20
25
30
35
40
45
50
55
60
65
70
Mass nr, N

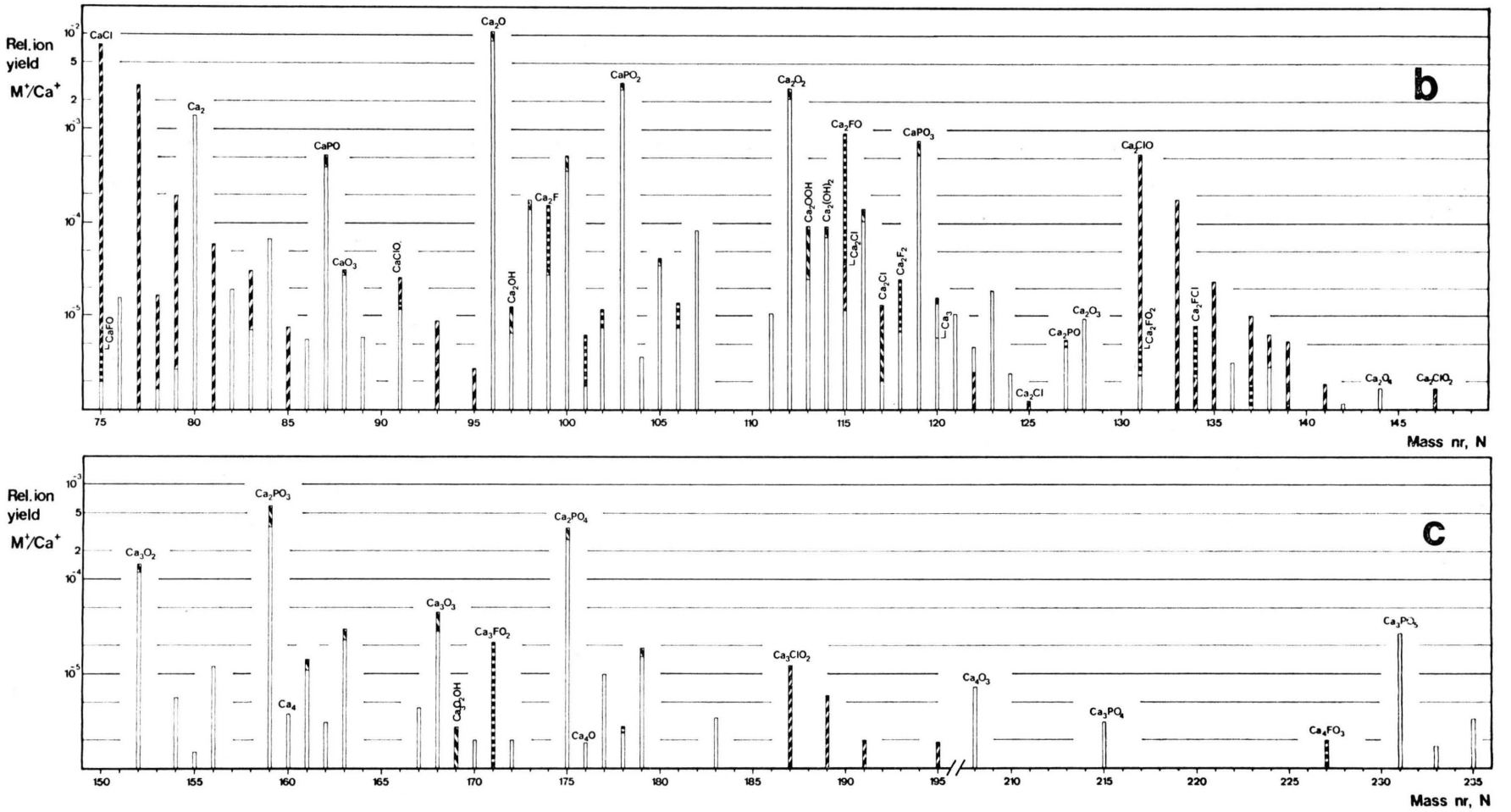

Fig. 1. Positive SIMS spectra of pure hydroxy-, fluor, and chlorapatite. a) Mass numbers 1—74; b) mass numbers 75—149; c) mass numbers 150—235.

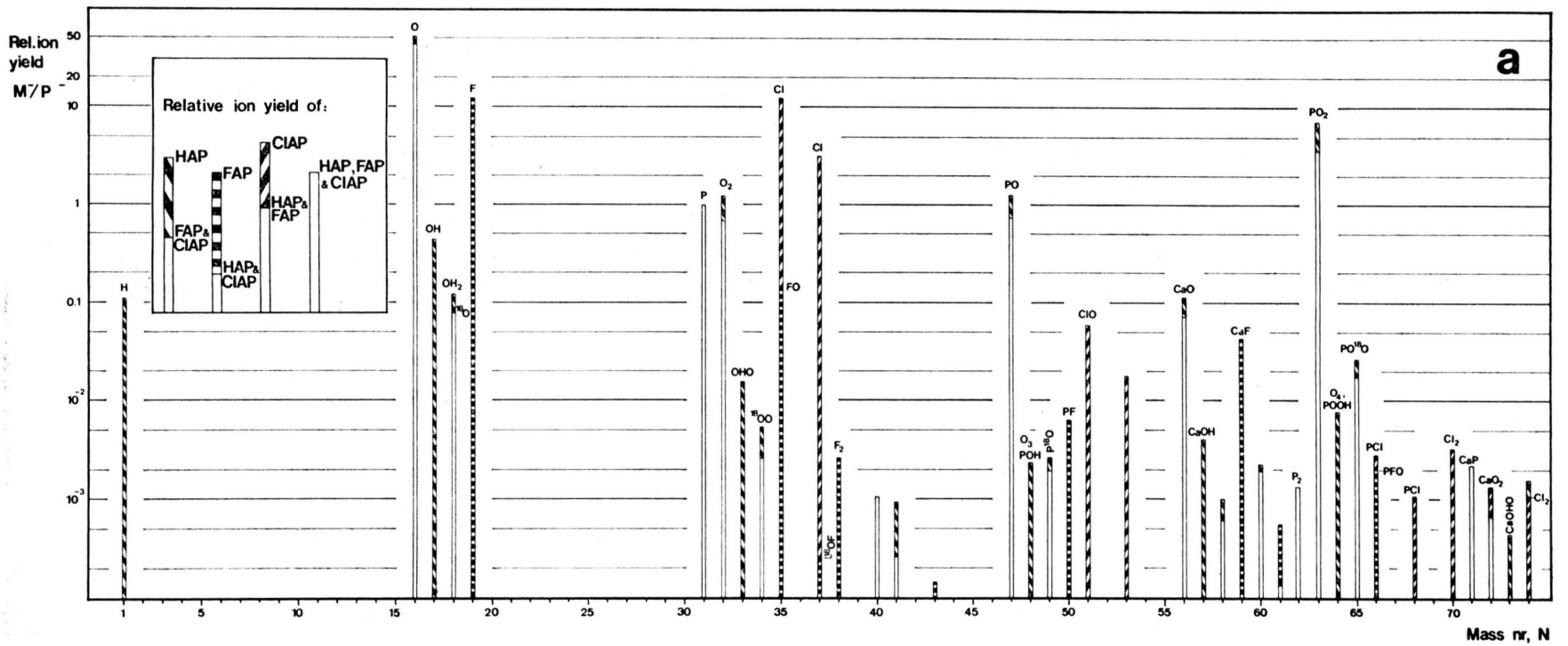

Fig. 2. Negative SIMS spectra of pure hydroxy-, fluor-, and chlorapatite. a) Mass numbers 1—74; b) mass numbers 75—130.

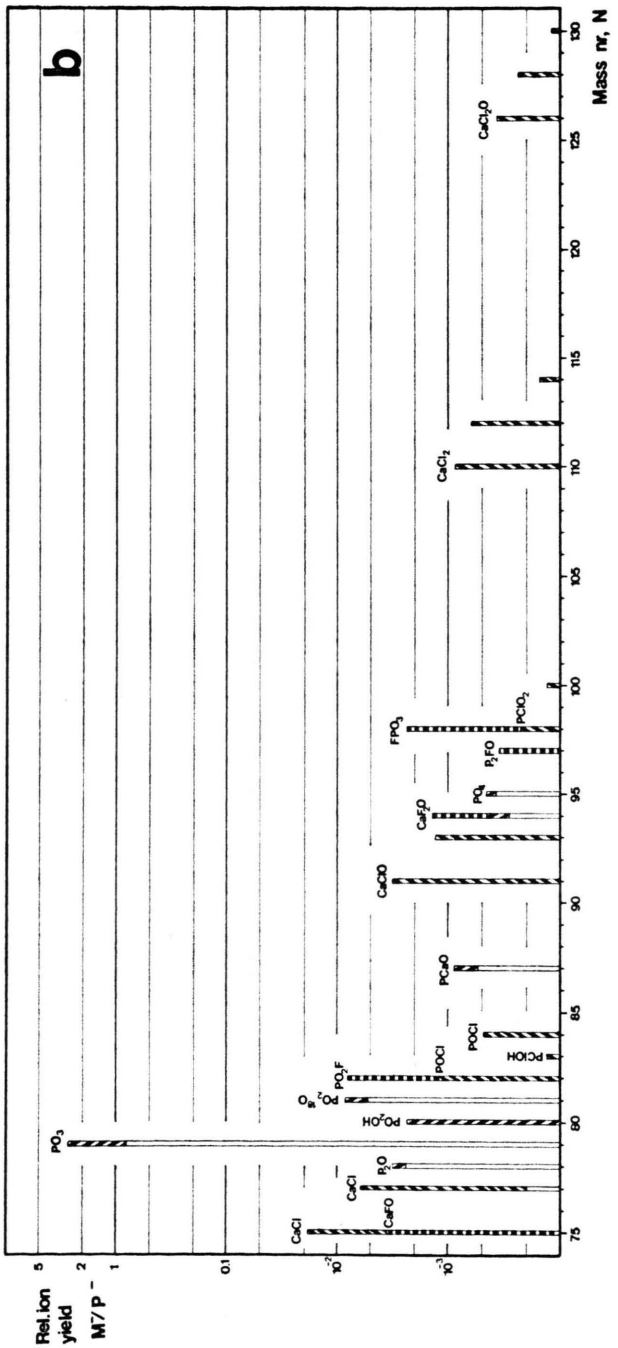

Fig. 2 b

are listed along with the major peaks in Tables 1 – 4. Observed small peaks are moreover taken into account in Tables 6 – 7, but only at such mass numbers that are relevant for trace element detection. In as far as these small peaks are known to be intrinsic, an equality sign applies in the "background" column; if other contaminants cannot be excluded, the inequality signs apply.

Tables 1 – 4 are intended to be mainly useful in the discussion of cluster and molecular ion formation. They therefore list the intrinsic peaks only for the most abundant isotope of each relevant species (i. e. containing only ^{40}Ca, ^{35}Cl, or ^{16}O). Other isotope peaks are neglected here. Instead, these are separately accounted for in Table 5, showing the expected isotope distribution of species containing one or several isotopic atoms. [An example of use of Table 5: If the peak height at $^{152}Ca_3O_2$ is A, then one expects on the 154 mass an isotope Ca_3O_2 contribution equal to $A \times \left(\frac{1.9}{91} + \frac{0.4}{99.5}\right)$.]

Tables 6 – 7 are of applied interest in trace-element analysis. For each element only such isotopes are listed whose mass numbers do not coincide with those of major intrinsic peaks (e. g. the main Fe isotope, 56, is not included becauses of the unavoidable CaO background). Very dilute isotope peaks are included only if, according to calculation (see Discussion), their use allows element detection in concentrations less than ca 10^3 ppm by weight. The "n" background level corresponds approximately to five times electronic noise.

Table 2. Hydrogen containing positive ion peaks in hydroxyapatite. Peak heights related to total Ca^+ yield. For minor (isotope) peaks, see Table 5. Note: quoted peak heights denote only approximate upper limits, as background hydrogen is always present as spectral contamination.

Ion species M	Main peak mass nr N	Relative yield M^+/Ca^+ ($\times 10^6$)
H^+	1	100
H_2^+	2	0.3
OH^+	17	6
CaH^+	41	150
$CaOH^+$	57	3000
Ca_2H^+	81	0.5
Ca_2OH^+	97	10
Ca_2OHO^+	113	85
$Ca_2(OH)_2^+$	114	40
$Ca_3OHO_2^+$	169	2.5

Table 3. Main F and Cr containing positive ion peaks in fluor- and chlorapatite, respectively. Peak heights related to total Ca^+ yield. For minor (isotope) peaks, see Table 5.

Ion species M	Main peak mass nr N	Relative yield M^+/Ca^+ ($\times 10^6$)	Ion species M	Main peak mass nr N	Relative yield M^+/Ca^+ ($\times 10^6$)
F^+	19	2800	Cl^+	35	690
F_2^+	38	2.0	Cl_2^+	70	$\leqq$0.2
FO^+	35	$\leqq$7	ClO^+	51	$\leqq$3
PF^+	50	31	PCl^+	66	$\leqq$3
CaF^+	59	28000	$CaCl^+$	75	8300
$CaFO^+$	75	$\leqq$15	$CaClO^+$	91	23
Ca_2F^+	99	130	Ca_2Cl^+	115	36
$Ca_2F_2^+$	118	20	$Ca_2Cl_2^+$	150	$\leqq$0.5
Ca_2FO^+	115	900	Ca_2ClO^+	131	550
$Ca_2FO_2^+$	131	$\leqq$3	$Ca_2ClO_2^+$	147	1.5
$Ca_3FO_2^+$	171	20	$Ca_3ClO_2^+$	187	12
$Ca_4FO_3^+$	227	$\leqq$2	$Ca_4ClO_3^+$	243	$\leqq$1

Table 4. Main peaks of intrinsic negative spectra. Peak heights related to $200\times P^-$ yield ($\approx$ total Ca^+ yield) Minor isotope peaks, see Table 5.

Ion species M		Main peak mass nr N	Relative yield $2\times10^8\ M^-/P^-$	Ion species M		Main peak mass nr N	Relative yield $2\times10^8\ M^-/P^-$
O^-		16	210000	F^-	(FAP only)	19	58000
O_2^-		32	3200	F_2^-	(")	38	15
O_3^-		48	4.6	F_3^-	(")	57	$\leqq$4
P^-		31	5000	FO^-	(")	35	700
P_2^-		62	7	PF^-	(")	50	50
PO^-		47	4600	PFO^-	(")	66	10
PO_2^-		63	19500	PFO_2^-	(")	82	43
PO_3^-		79	3800	PFO_3^-	(")	98	12
PO_4^-		95	1.7	CaF^-	(")	59	230
P_2O^-		78	1200	CaF_2^-	(")	78	$\leqq$10
$P_2O_2^-$		94	1.2	$CaFO$	(")	75	18
Ca^-		40	11	CaF_2O	(")	91	$\leqq$7
CaO^-		56	390	Cl^-	(ClAP only)	35	57000
CaO_2^-		72	28	Cl_2^-	(")	70	18
CaO_3^-		88	$\leqq$0.35	Cl_3^-	(")	105	$\leqq$0.11
Ca_2O^-		96	$\leqq$0.35	ClO^-	(")	51	300
CaP^-		71	11	PCl^-	(")	66	15
$CaPO$		87	2.8	$PClO^-$	(")	82	6.5
$CaPO_2^-$		103	$\leqq$4	$PClO_2^-$	(")	98	1.3
H^-	(HAP only)	1	$\leqq$500	$PClO_3^-$	(")	114	$\leqq$0.4
OH^-	(")	17	2300	$CaCl^-$	(")	75	90
OOH^-	(")	33	85	$CaCl_2^-$	(")	110	4
POH^-	(")	47	12	$CaClO^-$	(")	91	16
$P(OH)_2^-$	(")	64	35	$CaCl_2O^-$	(")	126	1.8
CaH^-	(")	41	$\leqq$4				
$CaOH^-$	(")	57	21				
$CaOOH^-$	(")	73	2.3				
$Ca(OH)_2$	(")	74	$\leqq$8				

The peaks where non-intrinsic background due to difficult-to-avoid hydrogen is likely to occur in practical analysis are indicated by "a" in the "remark" column. In the same column, "b" points out that useful analysis may be performed using a peak other than that of an element mass (an example is F, where the $^{59}CaF^+$ peak is about 10 times that of $^{19}F^+$; or La, where there is more LaO^+ than La^+). The "c" remark points out elements that can be detected more sensitively if the negative spectrum is used.

The D.S. column gives the order-of-magnitude concentration for each element to be "measurable" (criterium: ca five times background level) under

Table 5. Isotope peaks (expressed in percent of their sum) in dependence of the number (n) of Ca, Cl, or O atoms in the ionic species. N_0 denotes the mass numbers of atomic or cluster ions which contain exclusively the major isotopes (i. e. ^{40}Ca, ^{35}Cl, ^{16}O).

Mass number		N_0	N_0+1	N_0+2	N_0+3	N_0+4	N_0+6	N_0+8	N_0+12
Element	n								
Ca	1	97		0.65	0.145	2.05	0.0032	0.18	
Ca	2	94		1.25	0.28	4.0	0.033	0.39	0.0074
Ca	3	91		1.9	0.41	5.8	0.087	0.63	0.021
Cl	1	76		24					
Cl	2	58		36		5.8			
Cl	3	44		42		13.1	1.4		
O	1	99.8	0.04	0.20					
O	2	99.5	0.08	0.40	()	0.0004			
O	3	99.3	0.12	0.61	0.0005	0.0006	()		

Table 6. Element isotopes at mass numbers of low intrinsic spectral background in apatites. Positive spectrum. "n" denoting $M^+/Ca^+ \lesssim 10^{-7}$. Remarks: a) Peak likely to contain hydride, hydroxide or hydrocarbon contamination; b) Significant CaM^+ or MO^+ peaks in spectrum; c) Element peaks more dominant in negative spectrum (Table 6). "Detection sensitivity" D.S., I: <10 wt ppm; II: 10 to 100; III: 100 to 1000; () : >10^3 ppm.

Element	Isotope mass nr N	Abundance (%)	Background 10^6 M^+/Ca^+	Remark	D.S.
(H)	1	100	n (HAP $\approx 10^2$)	a,b,c	()
Li	7	92.5	n		I
Na	23	100	0.15		I
K	39	93.1	<0.5	a	I
Rb	85	72.2	<0.9 (ClAP$\leqq$8)		I
Cs	133	100	<0.9 (ClAP$\leqq$1.8)		I
Be	9	100	n		I
Mg	24	78.6	8.0		II
	25	10.1	<0.4	a	
	26	11.3	<0.4	a	
Sr	86	9.9	<0.5		II
	88	82.6	5.0		
Ba	137	11.3	0.9 (ClAP$\leqq$10)		I
	138	71.7	71.7		
Sc	45	100	<5	a,b	II
Y	89	100	<6	b	II
La	139	99.9	n	b	I
Ce	140	88.5	<0.5	b	I
Pr	141	100	<0.3 (ClAP 2.0)	b	I (II)
Nd	142	27.1	<1	b	I
	145	8.3	n		
	146	17.2	<0.3		
Sm	147	15.1	<0.4 (ClAP 1.6)	b	I
	148	11.3	<0.2		
Eu	151	47.8	<3.5	b	I
	153	52.2	<0.6		
Gd	157	15.7	<0.3	b	II
	158	24.9	1.1		
(Tb)				b	()
Dy	162	25.5	3.5	b	II
	164	28.2	0.5		
Ho	165	100	<0.6	b	II
Er	166	33.4	0.2	b	I
	170	14.9	<3.7		
Tm	169	100	<0.6	b	I
Yb	173	16.1	<0.4	b	II
	174	31.8	<0.9		
(Lu)				b	()
Th	232	100	0.3	b	II
U	238	99.2	n	b	I
Ti	46	8.0	35	a,b	III
	49	5.5	<7.9		
	50	5.3	<5.5		
Zr	90	51.5	1.9	b	II
	94	17.4	0.55		
Hf	178	27.1	<3.2	b	II
	180	35.4	0.4		
V	51	99.9	<0.7 (ClAP 3.4)		I (II)
Nb	93	100	<0.3 (ClAP 9.5)		I (III)
Ta	181	100	0.9		II
Cr	52	83.8	<10	a	II
	53	9.6	1	a	
Mo	92	15.9	0.75	b	II
	94	9.1	0.55		
	95	15.7	<3		
W	182	26.4	n	b	II
	184	30.6	<0.2		
	186	28.4	<0.4		
Mn	55	100	<1.2	a	II
Re	185	37.1	<0.15		II
	187	62.9	<0.3 (ClAP 12.0)		
Fe	54	5.8	0.5		III
Ru	101	17.1	<2 (FAP 6.0)		III
	102	31.7	<12		
Os	190	26.4	n (ClAP 0.2)		III
	192	41.0	n		
(Co)					()
(Rh)					()
Ir	191	37.3	n (ClAP 2.0)		II (III)
	193	62.7	n (ClAP 0.7)		

Continued Table 6

Element	Isotope mass nr N	Abundance (%)	Background 10^6 M^+/Ca^+	Remark	D.S.
(Ni)					()
Pd	108	26.7	3.7		III
	110	11..8	<0.6		
Pt	194	32.8	0.3		III
	195	33.7	*n* (ClAP 0.2)		
	196	25.4	*n* (ClAP 0.2)		
Cu	65	31	<8		III
Ag	109	48.7	1.3	c	III
Au	197	100	0.35	c	III
(Zn)					()
(Cd)					()
(Hg)					()
B	11	81.5	*n*		I
Al	27	100	<1	a	I
Ga	69	60.2	1		I
In	115	95.8	13 (FAP 910, ClAP 43)		II (III)
Tl	203	29.5	*n*		I
	205	70.5	<0.2		
C	12	98.9	<0.2	a,c	III
Si	28	92.3	<9	a,c	III
Ge	70	20.5	<0.7		III
	74	36.7	7.5		
Sn	118	24.0	7.0 (FAP 27.0)		III
	120	33.0	16		
Pb	206	23.6	<0.2		II
	207	22.6	<0.7		
(N)				c	()
(As)				c	()
(Sb)				c	()
Bi	209	100	<0.15		I
(S)					()
(Se)				c	()
(Te)				c	()
Fe	19	100	*n* (FAP 2700)	b,c	II
Cl	35	75.4	<1 (ClAP 680, FAP 7.0)	b,c	II
	37	24.6			
Br	79	50.5		b,c	III
	81	49.5			
I	127	100		b,c	III

above described standard experimental conditions of analysis. The arguments leading to the I-II-III-() classification are given in Discussion below. The most difficult-to-detect elements, marked with parentheses, are only included for completeness. Not included are only the noble gases, the matrix elements Ca, P and O, and all but two elements above the mass number 209.

Table 7. Element isotopes at low intrinsic spectral background, apatites; negative spectrum. "*n*" denoting $M^-/Ca^+ \lesssim 10^{-7}$ ($Ca^+ \cong 200\ P^-$). "Detection sensitivity", D.S., as in Table 6.

Element	Isotope mass nr N	Abundance (%)	Background 5×10^3 M^-/P^-	D.S.
H	1	100	*n* (HAP 5×10^3)	I
Ag	107	51.4	<0.2 (ClAP 0.5)	II
	109	48.6	*n* (ClAP 0.3)	
Au	197	100	*n*	II
C	12	98.9	<2	III
C_2	24	(98.4)	*n*	II
CN	26	(98.4)	<0.5	II
Si	28	92.3	<1	II
	29	4.7	*n*	
As	75	100	<2 (FAP 20, ClAP 100)	III
Sb	121	57.3	*n*	II
	123	42.7	*n*	
Se	80	49.8	<25	III
Te	128	31.8	*n*	II
	130	34.5	*n*	
F	19	100	<10 (FAP 6×10^4)	I
Cl	35	75.4	<1 (FAP 700, ClAP 5.6×10^4)	I
	37	24.6	<1 (ClAP 1.85×10^4)	
Br	81	49.5	<5	II
I	127	100	*n*	I

Discussion

a) Main Intrinsic Peaks

The investigated pure apatite material is characterized by the formula $Ca_5(PO_4)_3X$, where X stands for OH, F or Cl. The three types all form hexagonal or near-hexagonal (monoclinic) crystals, but differ significantly in properties like thermal stability, melting point and solubility. These differences are connected with the lattice space available for the X ion, the small F ion giving the least strained configuration [10].

In view of the wellknown importance of matrix effects in influencing SIMS ion yields, it is a positive surprise that the (calcium related) mass spectra of the three types of apatites turn out (see Figs. 1 – 2 and Tables 1 – 4) to be so similar. The peaks for ions not containing X or O are found to agree within about 10%. The O containing molecular ions (except O_2) all show the tendency to be somewhat more abundant for HAP than for FAP and ClAP. This is understandable, as the unit formula of the former contains 13 oxygen atoms, as compared to 12 in the

latter. The positive O and O_2 peaks do not exhibit this difference, which is not explicable by the oxygen from the primary beam; a control spectrum taken with N_2^+ instead of O^- as primary ion showed about the same 16 and 32 peak sizes. However, the positive oxygen ion yield is on account of high ionization potential expected to be very sensitive to "ionization temperature" T_i (see below), and the minor discrepancy is likely to be a secondary effect of the ionization mechanism.

In accordance with familiar thermodynamic models as well as with empirical experience [11 – 13, 2, 14] the ionization efficiency (in a given matrix) of each ionic species depends on an energy parameter kT_i, such that the ratio of ionized to non-ionized species in a sputtering cascade may be fairly well expressed as

$$\gamma^{\pm} = M^{\pm}/M^0 \simeq \text{const} \cdot \beta_M \cdot \exp\{E_M/kT_i\} . \quad (1)$$

For positive ions β_M is the ratio of the first excited state to ground state partition functions, and $E_M = \Delta E - E_i$, where E_i stands for ionization energy and ΔE for a correction term typical of the matrix. For negative ions β_M is the ratio of statistical weights, and $E_M = E_a$, the electron affinity. Because of the shortcomings of the present theoretical premises of the thermodynamic model, the "ionization temperature" parameter T_i is difficult to predict from first principles, and is by some workers routinely taken as typical for each particular matrix. This seems hardly justifiable, as the ionization efficiency has been shown to vary significantly even for a given element in a given matrix, depending on the conditions of bombardment (see, e. g., Ref. [4]). Some of the observed variations have probably been due to irreproducibility in the width and position of the energy window of the secondary ions. However, a considerable role also appears to be played by the crystallographic direction of the matrix. Preliminary studies of such effects have been carried out in connection with the present investigation. It was found that when the apatite crystal was rotated in relation to the primary beam, the greatest CaF^+/Ca^+ ratios were obtained at directions which also gave the greatest absolute Ca^+ currents. For P^+/Ca^+ the tendency was the opposite. The variations in M^+/Ca^+ could be as great as $\pm 50\%$ from the mean. Obviously, whatever may be the explanation of these directional effects, in quantitative analysis such variation must be taken into account. As shown in earlier publications [4, 14], a stoichiometry-independent indication of variations in the effective "ionization temperature" is available if check is kept of the Ca^{++}/Ca^+ or P^+/Ca^+ ratio.

The present spectra of polycrystalline HAP naturally correspond to ionization conditions at random crystal orientation. The single-crystal FAP and ClAP samples were oriented in such a way that the deviation from the $P^+/Ca^+ = 2.4 \times 10^{-3}$ value of HAP was less than 10% (and the corresponding difference in T_i less than ca 2%). It may thus be reasonably assumed that also the FAP and ClAP spectra do approximate the random orientation conditions.

The peaks containing F and Cl show, as expected, qualitatively similar tendencies. In accordance with Eq. (1), the high electron affinities of the halogens give rise to very high F^- and Cl^- peaks, the latter somewhat higher than the former in agreement with the corresponding difference in E_a. The knowledge of these peak heights and their variation with P^{+-}/Ca^{+-} (see Refs. [4, 14]) makes it possible to measure F and Cl concentrations quantitatively in the whole range of concentrations in $Ca_5(PO_4)_3(OH, F, Cl)$. This is likewise the case with the X^+ or CaX^+ peaks, and has been routinely applied in analysis [5, 4].

In the positive spectrum, however, the sizes of the F and Cl peaks are much too high to agree with the simple thermodynamic model. The fact that elements with high ionization potentials ($E_i \gtrsim 11$ eV) show disagreement with theory was pointed out by the first proponents of the model themselves [12]. Experience with apatites shows that the abundance of F^+ is as high as if the formation of the ion needed about 11 eV, instead of the tabled value of $E_i =$ 17.5 eV. It has been proposed [14] that F^+ is formed by a separation of the very abundant CaF^+ pair. This appears energetically plausible and also agrees with the fact observed in connection with the present study [8], that the energy distribution of F^+ ions is very similar to that of CaF^+.

As for the relative heights of the many intrinsic molecular and cluster peaks, their discussion (see also Ref. [7]) requires careful considerations of factors like binding energies and entropies, electron interactions, crystal structure and stoichiometry. This must be deferred to forthcoming publications.

b) Detectability of Impurities in Apatites

Despite the profusion, see Figs. 1 – 2, of high peaks characteristic of the pure matrix, many mass

numbers of low spectral background are available for the detection of trace impurities. In Tables 6 – 7 the elements are arranged groupwise according to the periodic table. For each element, the isotopes listed are the ones that exhibit the highest ratio of abundance to spectral background.

The assessment of "detection sensitivity", D.S., is made according to considerations of experimental ion yields for matrix elements, spectral background, isotopes abundance, and a simple model of the ionization mechanism.

Under the "standard" conditions of analysis (see preceding section) the total Ca^+ signal is found to lie 7 to 8 orders of magnitude above electronic noise. The noise level may be taken to be a theoretical detection limit, in the absence of spectral background. For an element with the same ionizability (γ^+) and mass number as Ca, this limit would lie at about 2×10^{-2} wt. ppm, as calcium accounts for ca 40% of the weight of apatite. For an element M with ionizability γ_M, regarding a peak of isotope mass m_M, abundance IA, this limit would accordingly be $2 \times 10^{-2} \times (\gamma_{Ca}/\gamma_M)(m_M/m_{Ca})(IA)^{-1}$ wt. ppm. In the presence of spectral background above electronic noise, this must be multiplied by $2 \times 10^7 \times M^{\pm}/Ca^+$, for which the fourth column of Tables 6 – 7 can be utilized. For real applications, a "practical limit for semiquantitative analysis" (PL) can be arbitrarily defined as 5 times the spectra background level, so that

$$(PL)_M = 2 \times 10^6 \times (M^{\pm}/Ca^+)\,(\gamma_{Ca}/\gamma_M) \cdot (m_M/m_{Ca})\,(IA)^{-1}\ (\text{wt. ppm})\,. \qquad (2)$$

The ionizability of each element could in principle be determined empirically from calibration samples of known composition. This would, however, entail arduous procedure, and can in practice only be done for a limited number of selected impurities. Hitherto only F, Cl, Mg, Sr, Na and La have been studied in this way [4, 14]. In the present assessment, recourse is instead taken to a rough simplification of the abovementioned thermodynamic model, which is known to give, for most elements, at least a correct order-of-magnitude prediction of γ [12, 14]. Thus, for the present purpose, the ratios [see Eq. (2)] of partition functions or of statistical weights are neglected. Further, it is assumed that $T_i \propto 8500\,K$, from the results of earlier studies on calibrated apatites [14]. Accordingly,

$$(PL)_M \approx 2 \times 10^6\,(M^{\pm}/Ca^+)\,(m_M/m_{Ca})\,(IA)^{-1} \cdot \exp\{(E_M - E_{Ca})/8500\,k\}\ (\text{wt. ppm})\,. \qquad (3)$$

The detectability classes I, II, III, () have been assigned in the D.S. column according to whether $(PL)_M$ lies below 10 wt. ppm, between 10 and 10^2, between 10^2 and 10^3, or above.

Naturally the use of an imperfect and simplified theoretical model entails great approximations. Nevertheless a notion can be obtained of the relative ease of detection of the individual elements. Roughly one may understand I as meaning "very easy to detect", II as "easy", III as "not easy in trace quantities" and () as "difficult".

As mentioned above, in some cases the application of the thermodynamic model should be particularly questioned. In the case of the halogens F and Cl, the D.S. in the positive spectrum is not based on the tabled E_i values, but on measured γ^+ values from calibration samples [4, 14]. In actual analysis, however, the CaF^+ and $CaCl^+$ peaks are normally used [5, 6], with D.S. in the I class.

In the case of elements exhibiting oxide peaks (remark "b" in Tables 6 – 7) the thermodynamic model is known [7, 14] to predict too great ion yields. For some of such elements the D.S. assignment in the Tables may therefore be one class on the low side. On the other hand, the study of the $(N+16)$ peaks offers additional detection possibilities.

The standard analyzing procedure used here does not exploit the full mass resolution obtainable by the apparatus. The D.S. assessments are based on the assumption that no spectral doublets are resolved. By careful adjustment of slits and at the cost of absolute ion intensity, $M/\Delta M$ ratios up to about 4500 can be achieved. This might facilitate special search for "difficult" impurities (e. g. ^{56}Fe, ^{59}Co, $^{64,66}Zn$, $^{116,118}Sn$).

Isotope "stripping" offers another means of lowering the practical limits for the analysis of certain elements. For example, the M^+/Ca^+ value, 35×10^{-6}, listed for ^{46}Ti, is due to the presence of $^{46}Ca^+$. The knowledge of the isotopic composition of Ca allows this contribution to be deduced from the other Ca^+ peak heights, and subtracted, leaving only less than 3×10^{-6} as effective background. Similarly the D.S. for Sr can be brought from II to I by computing the $^{88}Ca_2^+$ contribution from a measurement of $^{80}Ca_2^+$ (in practice by subtracting 0.4% of the 80 peak, see Table 5). Likewise, Mg can be brought into class I both by doublet separation and by the subtraction of $^{48}Ca^{++}$ from the 24 peak.

Even disregarding the additional possibilities available from isotope stripping, doublet separation, and the utilization of CaM or MO peaks, one may conclude from Tables 6 – 7 that at least 50 elements of the periodic table can easily be detected in apatite material even at concentrations smaller than 100 wt. ppm. For a number of elements, concentrations even below 1 ppm can be measured at least semi-quantitatively; among these are several of particular interest in bio- and geological apatite material, viz. all alkali metals, Mg, Sr, F and Cl.

It is borne out by the present study that, when wishing to perform a systematic element analysis of impurities in any matrix, among the principal requirements must be the careful charting of the total intrinsic spectra, as has been done here. A first assessment can in this way be made of the detectability limits of each element. Semi-quantitative analysis can often be performed by the aid of a theoretical model of the ionization mechanism. For quantitative analysis, the use of one external standard per element may be adequate, provided the parameters affecting variations in element ionizability are kept in check.

Acknowledgements

This work has been supported by the Patents Revenue Fund of Swedish Odontological Research and by the Swedish Natural Science Research Council. We are indebted to Dr. Gerrit Flim, Groningen, and to Dr. Jörgen Norén, Gothenburg, for providing apatite material.

[1] L. G. Petersson, G. Frostell, and A. Lodding, Z. Naturforsch. **29 c**, 417 (1974).
[2] A. Lodding, in "New Materials for Advanced Technical Applications", N. G. Ohlsson, ed., Stockholm 1977.
[3] A. Lodding, J.-M. Gourgout, L. G. Petersson, and G. Frostell, Z. Naturforsch. **29 a**, 897 (1974).
[4] S. J. Larsson, A. Lodding, H. Odelius, and L. G. Petersson, Calcif. Tiss. Res. **24**, 179 (1977).
[5] L. G. Petersson, H. Odelius, A. Lodding, S. J. Larsson, and G. Frostell, J. Dental Res. **55**, 980 (1976).
[6] G. Frostell, S. J. Larsson, A. Lodding, H. Odelius, and L. G. Petersson, Scand. J. Dent. Res. **85**, 18 (1977).
[7] A. E. Morgan and H. W. Werner, J. Chem. Phys., in press.
[8] H. Odelius, S. J. Larsson, and J.-M. Gourgout, to be published.
[9] M. Jarcho, C. H. Bolen, M. B. Thomas, J. F. Kay, and R. H. Doremus, J. Materials Sci. **11**, 2027 (1976).
[10] D. I. M. Knottnerus, Thesis, University of Groningen 1976.
[11] C. A. Andersen and J. R. Hinthorne, Anal. Chem. **45**, 1421 (1973).
[12] C. A. Andersen, in "Secondary Ion Mass Spectrometry", K. F. J. Heinrich and D. E. Newbury, eds., NBS Spec. Publ. **427** (1975).
[13] H. W. Werner, Vacuum **24**, 493 (1974).
[14] A. Lodding, contrib. to US-Japan SIMS Seminar, Hawaii 1975. To be published.